Journal for ImmunoTherapy of Cancer

MARC, a novel modular chimeric antigen receptor, improves T cell-based cancer immunotherapies by preventing early T cell exhaustion and enhancing persistence

Margaux Tual,[1,2] Angélique Bellemare-Pelletier,[2] Susan Moore,[2] Delphine Guipouy,[3] Negar Farzam-Kia,[3] Leila Jafarzadeh,[4] Jordan Quenneville,[2,5] Benoit Barrette,[6] Marc K Saba-El-Leil,[2] Jean-Sebastien Delisle ,[4] Etienne Gagnon [2,7]

To cite: Tual M, Bellemare-Pelletier A, Moore S, *et al*. MARC, a novel modular chimeric antigen receptor, improves T cell-based cancer immunotherapies by preventing early T cell exhaustion and enhancing persistence. *Journal for ImmunoTherapy of Cancer* 2025;**13**:e011829. doi:10.1136/jitc-2025-011829

► Additional supplemental material is published online only. To view, please visit the journal online (https://doi.org/10.1136/jitc-2025-011829).

MT and AB-P contributed equally.

Accepted 26 March 2025

For numbered affiliations see end of article.

Correspondence to
Dr Etienne Gagnon;
etienne.gagnon@umontreal.ca

ABSTRACT

Background Chimeric antigen receptor T cell (CAR-T)-based immunotherapies have reshaped the therapeutic landscape of cancer treatment, in particular for patients afflicted with leukemia. However, defects in CAR behaviors and clinical complications have hindered their widespread application across diverse cancer types. Chief among these defects is high tonic signaling, absent in native activating immune receptors, which accelerates T cell exhaustion and undermines treatment efficacy. We hypothesized that these limitations arise because current CAR architectures fail to replicate the modular design of native activating immune receptors, which integrate distinct receptor and signaling modules. This modular assembly is crucial for maintaining proper receptor regulation and function.

Methods Therefore, we set forth to develop a modular chimeric antigen receptor leveraging the same assembly principles found in native activating immune receptors to reestablish the intrinsic safeguards in receptor expression and signaling.

Results The resulting Modular Actuation Receptor Complex (MARC) displayed surface expression levels akin to its native immune receptor counterpart, the NK cell receptor KIR2DS3, while eliminating tonic signaling. In a clinically relevant mouse leukemia model, MARC-T cells exhibited remarkable long-term persistence and a less exhausted phenotype compared with conventional CAR-T cells.

Conclusions With its modular architecture, the MARC offers unparalleled opportunities for optimization and broad applicability across different cell types, paving the way for transformative advancements in cell-based therapies. This innovation holds immense promise as a next-generation therapeutic tool in clinical settings.

WHAT IS ALREADY KNOWN ON THIS TOPIC

⇒ Cell-based immunotherapies which make use of chimeric antigen receptors have revolutionized treatment for leukemia. However, current limitations, such as tonic signaling and rapid T cell exhaustion, limit the application of CAR-based therapies across different indications or applications.

WHAT THIS STUDY ADDS

⇒ The current study presents a novel chimeric receptor architecture, the Modular Actuation Receptor Complex (MARC), which recapitulates the native topology and functionality of activating and co-stimulatory receptors, thereby eliminating tonic signaling and improving T cell effector function and persistence.

HOW THIS STUDY MIGHT AFFECT RESEARCH, PRACTICE OR POLICY

⇒ This new modular receptor architecture is amenable to further development and optimization for use in a wide gamut of immune cell effectors. In addition, due to its lack of tonic signaling, the MARC could be compatible with HSC-based immunotherapeutic approaches.

INTRODUCTION

B-cell acute lymphoblastic leukemia (B-ALL) is the most common form of childhood leukemia, representing approximately 80% of cases.[1] The advent of chimeric antigen receptor (CAR)-T cell therapy has provided a transformative option for treating relapsed and refractory B-ALL. These therapies primarily target surface antigens such as CD19, CD20, and CD22, which are consistently expressed on malignant B cells.[2] However, despite their efficacy, CAR-T therapies face significant limitations that restrict their broader applicability across different cancers and demographics.

One major challenge with CAR-T cell therapy arises from the shared expression of target antigens, such as CD19, on both malignant and healthy B cells. The resulting

on-target, off-tumor activity leads to the long-term depletion of normal B cells, resulting in prolonged B-cell aplasia and subsequent lymphopenia, which severely compromises the patient's immune capabilities.[3] This problem is compounded in childhood leukemia due to the number of years the surviving patient would have to live without a fully functional immune system.[4] In addition, CAR-T therapies often induce serious immune-mediated toxicities, including cytokine release syndrome (CRS) and immune effector cell-associated neurotoxicity syndrome.[5] These complications increase the bedside costs and limit the deployment of CAR-T therapies for a broader patient population.[6]

Another significant limitation of CAR-T cells is the phenomenon of tonic signaling, which occurs when CARs are constitutively active in the absence of target engagement.[7] Whereas tonic signaling was shown to be beneficial in a few cases, in most cases it leads to premature exhaustion of T cells, reducing their ability to persist and function effectively in vivo.[8–10] The root of the discrepancies between native activating immune receptors and CARs likely lies in the overall design of CARs from the nature of scFvs, the hinge, and perhaps more importantly the juxtaposed costimulatory and activating signaling motifs.[8 9 11 12] Indeed, unlike the linear signaling architecture of current CARs, native immune receptors such as TCRs, BCRs, and NK cell activating receptors (NKRs) use multisubunit modular receptors consisting of distinct ligand-binding modules (RcMods) and signaling modules (SigMods).[13–19] These multisubunit receptors assemble via a simple yet effective process dictated by electrostatic interactions within the transmembrane (TM) regions enabling specific and high-affinity assembly, a process we have termed the transmembrane assembly registry (TAR).[20] This modularity provides critical safeguards, including stringent requirements for full receptor assembly before surface expression, resulting in lower basal expression levels and requiring discriminatory signaling on receptor engagement. Furthermore, the distribution of electrostatic charge across multiple cytoplasmic chains reduces steric hindrance during adaptor protein recruitment and facilitates trans-phosphorylation by Lck, ensuring proper signaling dynamics.[21–25]

In response to these challenges, we sought to design novel CARs to recapitulate normal immune receptor modular assembly and signaling kinetics, which could significantly improve treatment outcomes and mitigate current limitations and pitfalls observed in single-chain CAR technologies. To achieve this, we engineered synthetic TARs capable of driving specific receptor assembly and efficient surface expression. We further optimized the signaling capabilities of these receptors to provide robust activation signals while minimizing tonic signaling. Our resulting receptors, termed Modular Actuation Receptor Complexes (MARCs), displayed superior signaling outputs, minimal tonic signaling, and cytolytic activity toward target cells displaying lower target densities. In a preclinical model of CD19-positive leukemia, MARC-T cells eradicated leukemia more effectively than conventional 28ζ-CARs by preventing early exhaustion and promoting long-term persistence. These findings establish the MARC as a transformative synthetic signaling platform, offering significant improvements over traditional CAR designs and holding immense promise for advancing cell-based therapies.

RESULTS

Modular activating immune receptor components can be reprogrammed to drive differential assemblies

As a model immune receptor model for our study, we chose to use the NK cell activating receptor complex KIR2DS3/DAP12 (figure 1A). The electrostatic interaction found in this TAR is provided by residues K562 within the RcMod and D32 within the SigMod (figure 1B,C). To determine whether the KIR2DS3/DAP12 TAR could be re-engineered to accommodate the creation of a new activating immune complex without competing for endogenous components, we shifted the charged amino acid within the TARs of RcMod and SigMod by four positions in order to maintain the relative orientation of the charges within the TM scaffold.[26] The positional shifts were termed (4–) when toward the outer leaflet, and (4+) when they occurred toward the inner leaflet of the plasma membrane (figure 1B,C). We also shifted residue T566 in opposing fashion to that of K562 in order to maintain its putative role as stabilizing partner within the TAR.[27] Interestingly, changing the positioning of these key amino acids greatly modified, in some cases, the hydrophobic profile of the TM domains within the RcMod and SigMod (figure 1B,C). With this approach, we produced a small library of RcMod and SigMod containing various TARs and cloned each library in vectors containing different fluorescent reporters, with the RcMod library coexpressing mCherry and the SigMod library coexpressing ZsGreen. Jurkat T cells were then cotransduced at multiplicity of infection (MOI) 0.5 (figure 1A). To determine the efficiency at which the combination of RcMod and SigMod enabled receptor assembly and surface expression, cells were stained with Alexa647-labeled anti-KIRD2DS3 and then analyzed by flow cytometry (figure 1D). The dual reporter approach also allowed us to monitor RcMod leakiness, that is, surface expression in the absence of the SigMod, by gating on mCherry (mCH) only cells, whereas gating on the ZsGreen (ZsG) only cells acted as a negative control (figure 1B). For each RcMod variation, we calculated the assembly factor, that is, the increase in surface expression when co-expressed with a given SigMod, and measured leakiness.

As expected, the WT RcMod was minimally expressed at the surface when expressed by itself and displayed a substantial increase in surface expression when coexpressed with the WT SigMod but failed to assemble with charge-shifted SigMods (figure 1D,E, online supplemental figure S1B). Interestingly, although the 4+RcMod showed a small but significant increase in leakiness compared

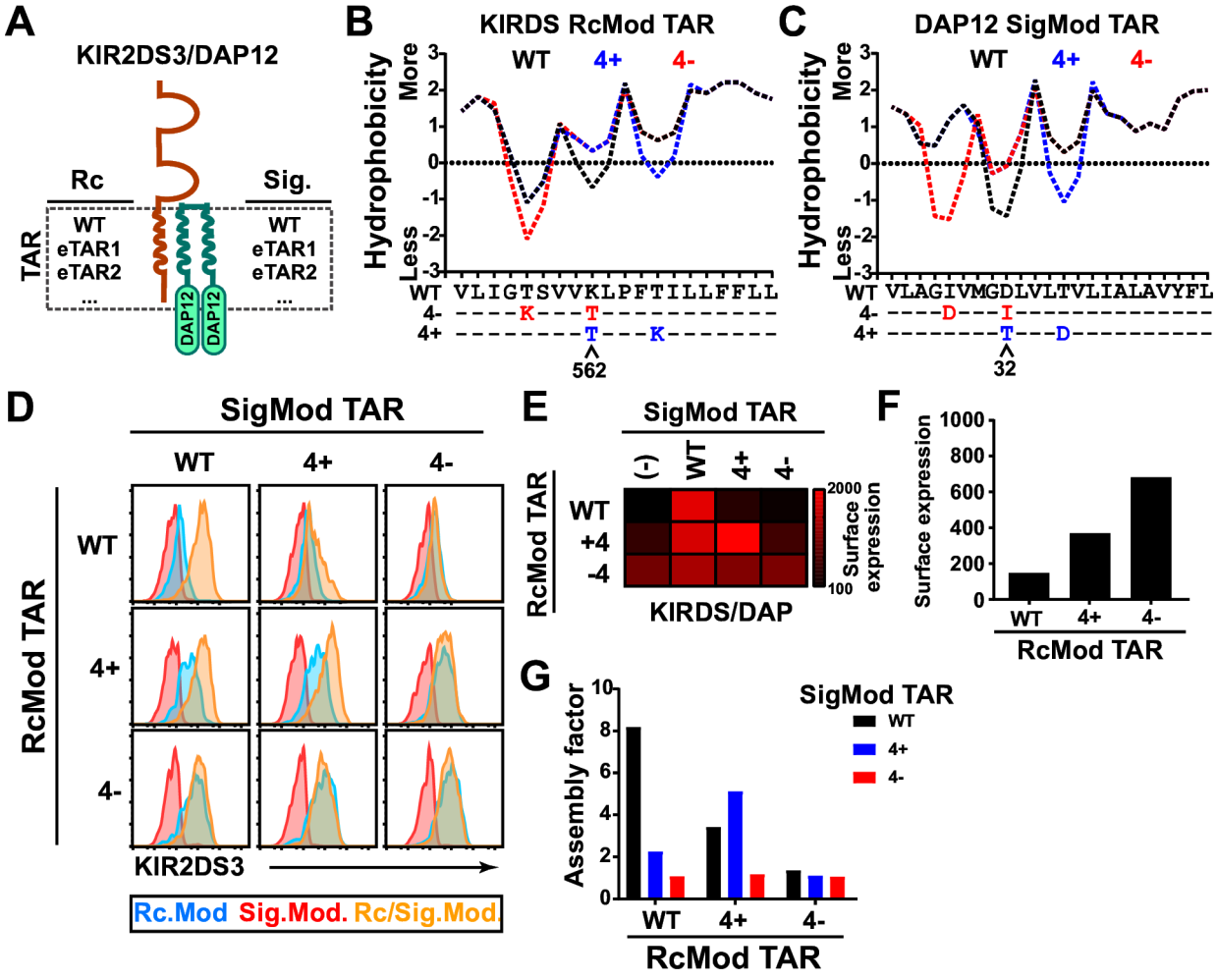

Figure 1 Reprogramming of modular receptor TARs. Jurkat T cells were cotransduced to express the indicated RcMods and SigMods. Stably expressing cell lines were analyzed for RcMod surface expression in the presence or absence of SigMod. Data shown are representative of four independent experiments. (A) Schematic of the different components that make up the modular immune receptor KIR2DS3 representing the RcMod and DAP12 representing the SigMod. The TAR is indicated as well as the engineered TARs (eTAR) used for the screening. (B) Hydrophobicity profile of the RcMod transmembrane domain encompassing the TAR for each of the TARs tested. The position of the original charged residue is indicated. (C) Hydrophobicity profile of the SigMod transmembrane domain encompassing the TAR for each of the TARs tested. The position of the original charged residue is indicated. (D) FACS plots displaying surface expression of the various modular immune receptors created by different combinations of RcMod and SigMod. Cells were stained with APC-labeled anti-KIR2DS3 antibody. Subpopulations containing RcMod only, SigMod only, or both are indicated. (E) Heatmap displaying surface expression levels of the various RcMods tested in the absence or presence of SigMods. (F) RcMod leakiness as determined in the RcMod only population according to the various TARs tested. (G) Assembly-dependent increase in surface expression for each RcMod and SigMod combination was calculated and is displayed as assembly factor. TAR, transmembrane assembly registry.

with that of its WT counterpart, it could still assemble with both the WT and 4+SigMod, although more effectively with the 4+SigMod (figure 1F,G). Conversely, the 4–RcMod displayed high levels of leakiness, with minimal ability to assemble with any of the SigMods tested. Together, these results indicate that the positional charges that enable the formation of the TAR are the main driver of immune receptor assembly. Of note, the 4–SigMod did not assemble productively with any of the RcMods, and in some cases caused a reduction in RcMod surface expression, indicating that it was deleterious to receptor stability within the membrane (figure 1G). These findings were confirmed with another model immune receptor complex NKG2D/DAP12, where the RcMod is found as a type II TM protein (online supplemental figure S1C-E).

Modular receptor TM domains only require charged residues for assembly

To better characterize the elements that regulate RcMod leakiness, we created synthetic TARs comprised entirely of leucines (pL) from G557 to I567 using the KIR2DS3 TAR as the starting point and positioning the lysine to recapitulate either the WT (pL0) or shifted positions (pL4+, pL4–) assessed earlier. We also generated RcMods that contained two lysines; one at position "0" and the other at the shifted position (pL4-K, pL4+K) due to the

previously observed leakiness of the 4+ and 4–RcMods (figure 2A). While the pL0 and pL4+RcMods preferentially assembled with their registry-matched SigMod, they also displayed significant leakiness (figure 2B,C). Also, as previously observed for the 4–RcMod, the pL4–RcMod displayed significant leakiness, and surface expression was not increased when coexpressed with any of the SigMods (online supplemental figure S2A). Contrastingly, in both pL4+K and pL4-K RcMods, leakiness was greatly reduced (figure 2B,C, online supplemental figure S2A). Moreover, while both of them could assemble with WT SigMod, assembly of the pL4+K RcMod with its registry-matched SigMod was significantly enhanced (figure 2B,C, online supplemental figure S2B). Together, these results suggest that although the relative positions of the charged amino acids within the TM of each module are critical, they remain somewhat permissive for receptor assembly in mismatched TARs. This also suggests that overall TAR hydrophobicity of the RcMod dictates its leakiness.

To test this, we performed a mutagenesis screen at the "0" position within the pL4+TM domain. We chose a variety of non-hydrophobic, hydrophobic, and aliphatic amino acids with different hydrophobic indexes (H.I.) giving rise to a variety of TM hydrophobic profiles (figure 2D, online supplemental figure S2C).[28 29] Individual RcMods were transduced either in WT Jurkat T cells or in cells already expressing the 4+SigMod followed by measurement of RcMod leakiness and assembly-dependent surface expression (figure 2E,F). Except for histidine, there was a clear correlation between the hydrophobicity index of the amino acid at position "0" within the TAR and leakiness, suggesting that poorly hydrophobic TM domains enabled retention or degradation of the RcMod in the absence of SigMod (figure 2G). Indeed, when histidine was included at position "0", the RcMod was efficiently retained from surface expression despite having a mid-range hydrophobicity index and facilitated SigMod-dependent assembly and surface expression (figure 2G,H, online supplemental figure S2C). Interestingly, the pL4+H RcMod was more discriminatory than pL4+K for it ability to assemble with Registry-matched SigMod as it was unable to assemble with the WT SigMod (figure 2F, online supplemental figure S2D).

Reprogrammed modular receptors are superior at activating antigen-specific receptors

Next, we tested whether the novel reprogrammed modular receptors could be used as CARs and whether signaling could be optimized. To do so, we first modified the extracellular portion of the KIR2DS3 extracellular domain by truncating the distal Ig domain and replacing it with the CD19-targeting single-chain variable fragment derived from the FMC63 antibody (online supplemental figure S3A). We chose to use the CD19-targeting scFv because of its reduced propensity to induce interchain refolding. The remaining CAR-dependent tonic signaling enables us to characterize the impact of remodeling the cytoplasmic topologies of the activating and costimulatory components of the CAR within the RcMod and SigMod of the MARC on receptor architecture-based tonic signaling. We tested various RcMod TARs, namely the WT, the 4+ and the pL4+K (hereafter named RS for RcMod synthetic TAR) for their ability to assemble with SigMods containing either the WT or 4+ (hereafter named DS for DAP12 synthetic TAR) TARs. We also compared the activating potential of either the DAP12 (D) or CD3ζ (Z) cytoplasmic domain (CytoD) in Jurkat T cells. As observed previously, all RcMods tested maintained their assembly specificity and requirement for efficient surface expression, indicating that modification of the extracellular portion of the receptor had no effect on the underlying mechanisms of assembly (figure 3A, online supplemental figure S3B).

To determine the activation potency of these MARCs on target cell recognition, we incubated the MARC-expressing Jurkat T cell lines with or without Toledo cells, a CD19+patient-derived B cell lymphoma, overnight followed by CD69 staining and flow cytometry analyses (figure 3B).[30] No CD69 surface expression was detected in the absence of target cells, indicating that these receptor architectures did not provide high tonic signaling, contrary to what was previously observed for other 28Z-CARs (figure 3C,D).[12 31 32] When target cells were added, all MARC-expressing Jurkat-T cells displayed significant surface expression of CD69 (figure 3C,D). Registry matching of the 4+ and RS RcModules with the DS SigMods resulted in an increase in activation, as determined by relative abundance of CD69+ cells. Also, except for the WT RcMod conditions, there was a clear increase in activation potential when comparing the DSD and DSZ pairings with either the 4+ or RS RcMod, indicating a clear impact of the number of ITAMs (Immunoreceptor Tyrosine-based Activation Motifs) on activation. This resulted in a near fourfold increase in cell activating potential for the RS and DSZ pairing when compared with the native KIR2DS/DAP12 (WT/WT) used in previous studies, making this MARC a prime candidate for benchmarking (figure 3C, online supplemental figure S3B).[27]

Next, we benchmarked these novel MARCs against clinically relevant CARs from first generation containing CD3ζ only (Z) and second generation containing both the CD28 and CD3ζ signaling moieties (28Z) (figure 3D). To do so, we first changed the hinge domain of the RcMod to CD8α to match that of the tested CARs and added or not the CD28 cytoplasmic domain to generate MARC equivalents for first and second generation CARs (figure 3D). We also included the WT KIR2DS3/DAP12 (DD) receptor for comparison, as several iterations of this receptor had been tested as CARs in various effector cells.[27 33] We cloned the different CD19-MARCs as 2A fusion protein to drive the expression of both components by a single promoter. Cells expressing the 2A version of the MARC displayed a small but statistically insignificant reduction of surface-expressed receptor and target cell-dependent activation, and neither of the CD19-MARC configurations

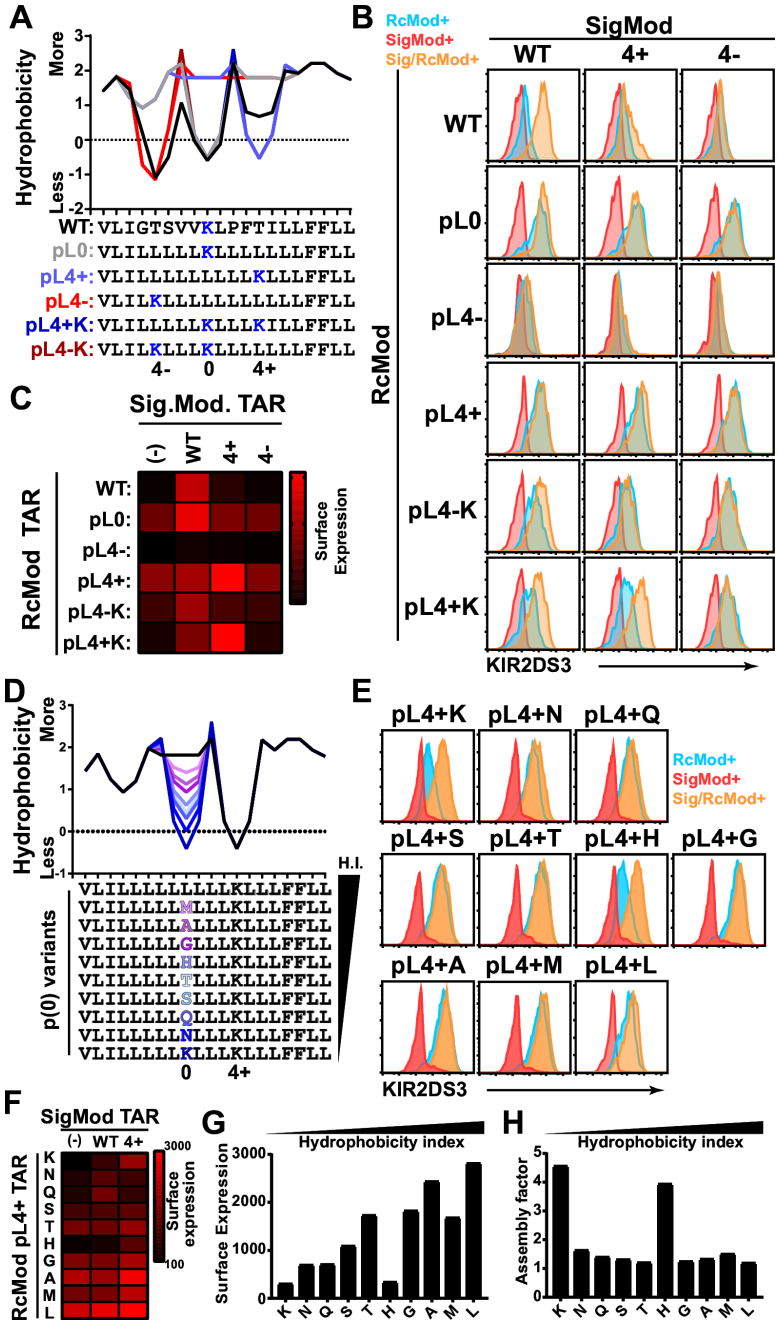

Figure 2 Impact of TM identity and charge positioning in TARs on receptor assembly and leakiness. Jurkat T cells were cotransduced to express the indicated RcMods and SigMods. Stably expressing cell lines were analyzed for RcMod surface expression in the presence or absence of SigMod. Data shown are representative of four independent experiments. (A) Hydrophobicity profile of the RcMod transmembrane domain encompassing the TAR for each of the RcMod TARs tested. The position of the original lysine residue is indicated as 0, while registry-shifted lysine residues are indicated as 4– or 4+. (B) FACS plots displaying surface expression of the various modular immune receptors created by different combinations of RcMods and SigMods tested. Cells were stained with APC-labeled anti-KIR2DS3 antibody. Subpopulations containing RcMod only, SigMod only, or both are indicated. (C) Heatmap displaying the surface expression levels of the various RcMods tested in the absence or presence of SigMods. (D) Hydrophobicity profile of the RcMod transmembrane domain encompassing the TAR for each of the RcMod TARs tested. The position of the original charged residue is indicated as 0, while the registry-shifted charged residue is indicated as 4+. (E) FACS plots displaying surface expression of the various modular immune receptors created by different combinations of RcMods and SigMods. Cells were stained with APC-labeled anti-KIR2DS3 antibody. Subpopulations containing RcMod only, SigMod only, or both are indicated. (F) Heatmap displaying the level of surface expression of the various RcMods tested in the absence or presence of various of SigMods tested. (G) RcMod leakiness as determined in the RcMod only population according to the various TARs tested. Amino acids presented on the x-axis are ordered according to their hydrophobicity index. (H) Assembly-dependent increase in surface expression for each RcMod and SigMod combination was calculated and is displayed as assembly factor. Amino acids presented on the x-axis are ranked according to their hydrophobicity index. TAR, transmembrane assembly registry; TM, transmembrane.

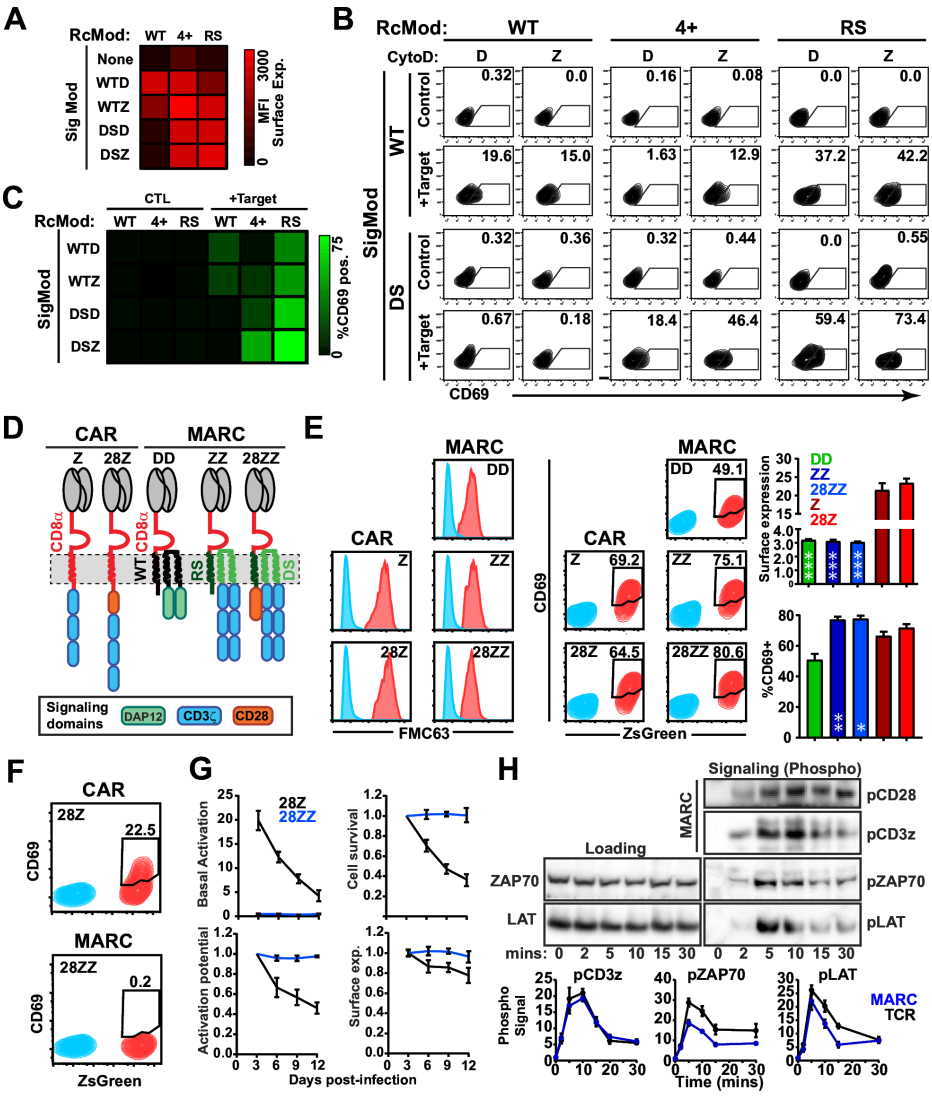

Figure 3 Signaling optimized Modular Activating Receptor Complexes (MARC) recapitulate immune receptor behaviors. Jurkat T cells were transduced with the constructs detailed in online supplemental figure 1A and tested for surface expression of the receptors and their ability to activate following coincubation with CD19-expressing target cells. (A) Heatmap displaying the surface expression levels of the various RcMods tested in the absence or presence of SigMods. (B) Example of flow cytometry analysis and CD69 gating used to generate the data presented in C. Experiment is representative of four experiments. SSC-H is plotted on the y-axis. (C) Heatmap displaying the level of cell activation of the various RcMods tested in the absence or presence of SigMods, as identified by the percentage of CD69-positive cells following an incubation in the absence or presence of CD19-expressing target cells. Data shown are representative of four independent experiments. (D) Schematic representation of the various CARs (Z, 28Z) and MARCs (DD, ZZ, 28ZZ) used for the assays. (E) Left: FACS analyses of surface expression of the CARs and MARCs presented as histograms of anti-FMC63 staining. Center: FACS analyses of activation status of the various cell lines expressing CARs or MARCs as determined by CD69 surface staining following coincubation with target cells. Red: ZsGreen positive, CAR or MARC-expressing Jurkat cells. Blue: ZsGreen negative (WT) Jurkat T cells. Right: recapitulative analyses of surface expression of the CARs and MARCs and activation potencies. ZsGreen+cells: red; WT Jurkat T cells: blue, N=5. Error bars indicate SEM. Significance was determined using two-way ANOVA with multiple comparisons, using Tukey post hoc test. Statistical significance for surface expression was established between indicated MARC and either of the CARs. Statistical significance of relative abundance of CD69+cells was determined between matched MARC/CAR depending on their signaling composition. (F) Tonic activation status of the 28Z-CAR and 28ZZ-MARC as determined by the expression of surface CD69, in the absence of target cells. ZsGreen+cells: red; WT Jurkat T cells: blue. (G) Jurkat T cells were transduced with either 28Z-CAR or 28ZZ-MARC and were repeatedly stimulated over the course of 12 days with NALM6 cells. Cells were analyzed for tonic activation (% of CD69+cells), cell survival (relative ratio of ZsGreen positive cells vs day 3), activation potential (relative ratio of CD69-positive cells vs day 3) and receptor surface expression every 3 days (relative ratio of anti-FMC63+cells vs day 3). (H) Top: 28ZZ-MARC expressing Jurkat T cells were co-incubated with Tax-Lact-C2-RFP-JY1 cells for the indicated period of time. Following this, cells were lysed and analyzed for MARC-dependent signaling using Western blot analyses. Bottom: recapitulative and comparative analyses of MARC and TCR-dependent signaling kinetics. Phospho signals were normalized to loading control for three separate exposure times. Data are representative of three separate experiments. ANOVA, analysis of variance.The p values are indicated as ns: non significant, ≤0.05: *, ≤0.01:**; 0.001:***.

induced significant basal activation (online supplemental figure S3D–F).

Compared with both generations of CARs (Z, 28Z), all three MARCs (DD, ZZ, 28ZZ) displayed highly reduced surface expression 3 days post-transduction (figure 3E). However, with the exception of the DD-MARC, all receptors were able to robustly activate the cells following stimulation with CD19-expressing target cells (figure 3E). As expected, the Jurkat T cells expressing the 28Z-CAR, known to provide high tonic signaling, displayed high basal activation, whereas the Jurkat T cells expressing 28ZZ-MARC did not (figure 3F). This trend was observed in all 28Z-CARs tested but was exacerbated in CAR constructs containing scFvs known to promote interchain refolding, such as those targeting GD2 and CD33.[8 11] Nevertheless, the MARC equivalent displayed little to no tonic signaling with all scFvs tested (online supplemental figure S3G). Because of this, we investigated the effects of basal activation in the context of the CD19-targeting 28Z-CAR or 28ZZ-MARC. Cells transduced with either receptor were analyzed every 3 days over the course of 12 days for their basal activation status, as well as for their ability to survive and to maintain activation potency and receptor expression. The 28Z-CAR expressing cells had a significant proportion displaying basal activation on day 3, which diminished over the course of 12 days. This reduction in basal activation coincided with a reduction in cell survival, activation potency, and CAR surface expression, clearly highlighting the deleterious effects of high tonic signaling and activation on the cells (figure 3G, online supplemental figure S3H–K). On the other hand, the 28ZZ-MARC expressing cells maintained a non-activated resting state and high cell viability, activation potential, and receptor surface expression suggesting low to no basal signaling.

To validate this and to gain insights into the signaling dynamics of the 28ZZ-MARC, we performed a signaling kinetic assay using Tax-Lact-C2-RFP-JY1 (TJY) cells, which have high surface expression of CD19 as well as the HTLV-derived Tax peptide recognized by the A6 TCR as described in our previous work.[34] MARC or A6-Jurkat T cells were stimulated with TJY cells, lysed, and then processed for Western blot analyses. Contrary to what is known about CARs, the 28ZZ-MARC did not display any basal phosphorylation (figure 3H). However, following target recognition, MARC components (CD28 and CD3ζ) and downstream effectors (ZAP70 and LAT) were rapidly and efficiently phosphorylated. Signaling kinetics for CD3ζ, ZAP70, and LAT were similar to those observed following TCR recognition of cognate pMHC (figure 3H).[12 32 35] Conversely, signaling kinetics of the CD28 moiety within the MARC were more sustained than the CD3ζ moiety of the MARC (online supplemental figure S3J). These results suggest that the recapitulation of the normal cytoplasmic topologies of both activating and costimulatory receptors within the modular nature of the MARC provides similar signaling potencies and kinetics to their native counterparts, resulting in prolonged MARC-T cell funcionality.

Primary MARC-T cells are efficient at killing low-density target cells through stable immune synapse formation

Considering the potency and dynamics of MARC signaling, we next tested whether this translated into enhanced functionality in primary human T cells. We expanded primary T cells from PBMCs and transduced them to express the 28Z-CAR (CAR) or 28ZZ-MARC (MARC), or ZsGreen only (Mock). As observed in Jurkat T cells, CAR surface expression was greater than that of the MARC, despite the cells showing a reduced ZsGreen signal (figure 4A, online supplemental figure S4A). Despite evident tonic signaling in CARs, there were no significant differences in CD4:CD8 ratios, memory phenotype, nor exhaustion status between CAR-T cells and MARC-T cells following in vitro expansion (online supplemental figure 4B–D). It is important to note, however, that following T cell expansion according to our culture conditions, all T cells expressed low levels of Tim3. For this reason, we considered Tim3-Hi cells as more indicative of exhaustion (figure 4D). We next investigated receptor behavior following target cell recognition. For this, we stimulated CAR-T cells and MARC-T cells with target cells (NALM6-mCherry) and monitored receptor surface expression (online supplemental figure S4E). Here again, we observed no statistical significance between them, as both receptors were efficiently internalized following stimulation (figure 4B). Finally, CAR and MARC-T cells displayed similar functional avidity to NALM6 cells, even though MARC-T cells express roughly four times fewer receptors at the surface (figure 4C, online supplemental figure S4F). Together, these results suggest that MARCs are more potent as receptors than CARs and that MARC-T cells may not require as much ligand to engage their effector functions.

While CAR-T cells and MARC-T cells were equally capable of killing high target density NALM6 cells at various E:T ratios, cytolytic activity toward cells that present lower density targets was greater for MARC-T cells (figure 4D, online supplemental figure S4G,H). Lack of cytotoxicity toward Jurkat T cells, which do not express CD19, and T cells only expressing the RcMod indicate that the observed difference in cytotoxicity toward lower target densities was not due to non-specific killing. Moreover, lack of cytolytic activity in T cells expressing only the RcMod validates the lack of aberrant assembly with endogenous receptors and a necessity for the registry-matched SigMod for efficient surface expression and function (online supplemental figure S4H).

Finally, we looked at whether the MARC-T could form stable immune synapses following target recognition, as it is well established that CAR-T cells form transient cell–cell interactions with target cells, also known as

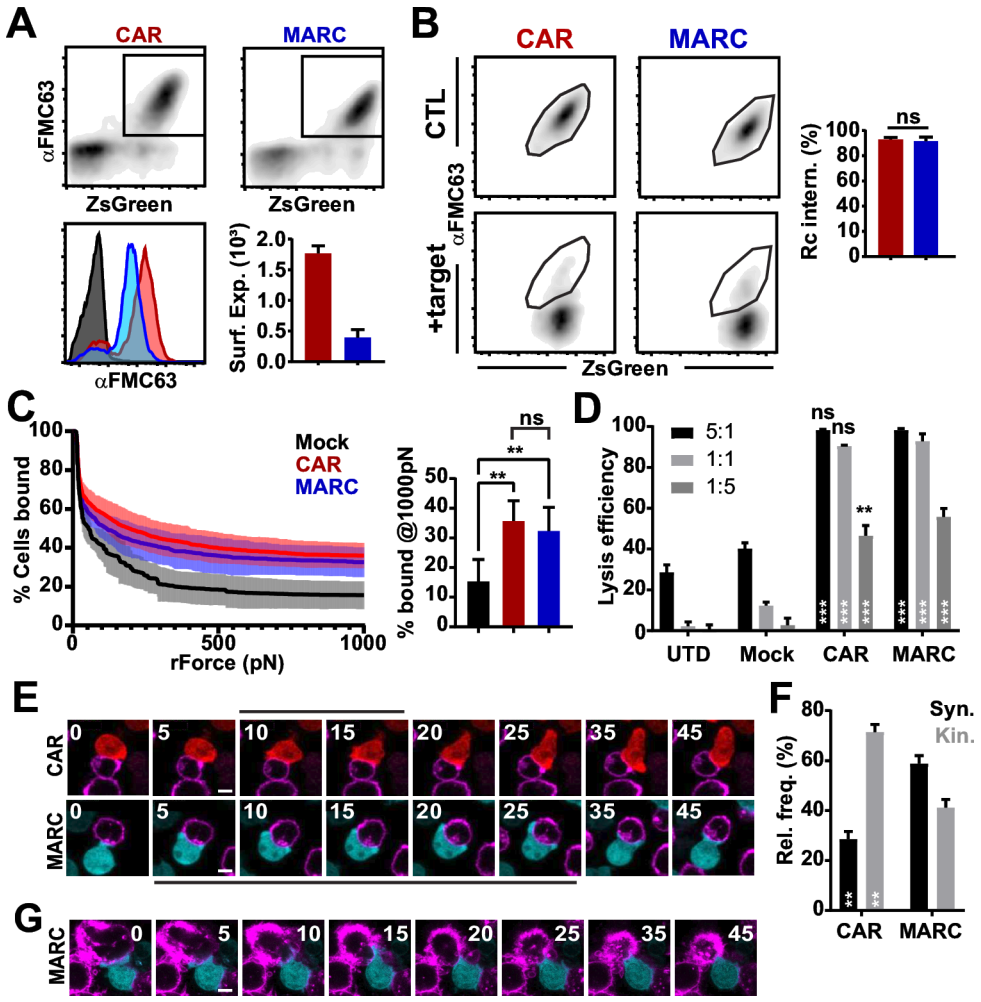

Figure 4 MARC-T cells form stable immune synapses and efficiently kill tumor cells. Primary human T cells were stimulated, transduced with either ZsGreen (control), CD19-targeting 28Z-CAR (CAR) or 28ZZ-MARC (MARC) expanded for 8 days and analyzed. (A) Top: FACS analyses of transduction efficiencies and surface expression of the CAR and MARC. Bottom left: FACS histograms displaying differential surface expression of the CAR (red) or MARC (blue) after staining the cells with anti-FMC63. Bottom right: surface expression of the MARC or CAR from three separate transductions of primary T cells. Surface expression is presented as arbitrary units. Untransduced cells are presented in gray. (B) Left: FACS plots displaying surface expression of the CAR and MARC receptors as determined by anti-FMC63 staining in ZsGreen+cells, before and after overnight incubation with the NALM6 target cells. Right: relative receptor internalization efficiencies following target cell co-incubation. N=3. (C) Functional avidity determination. NALM6 cells were loaded onto the Lumicks flow cells and left to adhere for 30 min. Following this, control or CD19-targeting CAR or MARC-T cells were added and left to interact for 5 min. Cells were then analyzed for functional avidity using the standard approach. Left: relative abundance of T cells attached to NALM6 cells at various resonance intensities in piconewtons. Right: relative abundance of cells still attached to NALM6 cells at 1000 piconewtons. Statistical significance was determined using two-way ANOVA with multiple comparisons, using Tukey post hoc test. N=3. (D) Untransduced (UTD), ZsGreen only (Mock), CD19-targeting CAR or MARC-T cells were coincubated with mCherry-NALM6 cells at different effector:target ratios (E:T) for 24 hours, and relative cytolysis of mCherry-NALM6 cells was assessed by FACS. Statistical significance was determined using Two-WAY ANOVA with multiple comparisons, using Tukey post hoc test. N=3. Statistical significance between CAR or MARC versus Mock is indicated within the bars, differences between CAR and MARC are displayed above the bars. (E) CD19-targeting CAR and MARC-T cells were mixed with JY cells expressing LactC2-mRFP in a flow cell chamber at a ratio of 1:5 and imaged over the course of 60 min. Effector (E) and target (T) cell conjugates were scored for synapse or kinapse formation based on the duration and morphology of the contact. The black line indicates stable contact between E:T, the white line represents 10 µm, and the numbers indicate the minutes after initial E:T contact. (F) Cumulative analyses of synapse and kinapse formation between CAR (red) or MARC-T (cyan) cells and Toledo cells (magenta) as determined by images acquired in E. A minimum of 50 cells were used per condition. Statistical significance of synapse or kinapse formation between CAR and MARC was determined using two-way ANOVA with multiple comparisons, using Sidak post hoc test. N=3, minimum 15 synapses per N. (G) MARC expressing CD8 T cells (cyan) were sorted and mixed with Toledo cells expressing LactC2-mRFP (magenta) in a flow cell chamber at a ratio of 1:5 and imaged over the course of 60 min. Images show an example of a single MARC-T cell attacking and killing a target Toledo cell over the course of imaging. ANOVA, analysis of variance; MARC, Modular Actuation Receptor Complex. The p values are indicated as ns: non significant, ≤0.05: *, ≤0.01:**; 0.001:***.

kinapses.[36–38] CAR and MARC-T were stimulated with Lact-C2-RFP Toledo cells and imaged for 60 min. CAR-T cells and MARC-T cells that interacted for a prolonged period of time (minimum of 5 min) were monitored for their ability to form stable synapses or kinapses with their target cell (figure 4E). We found that MARC-T cells primarily formed stable synapses with their target, while CAR-T primarily formed kinapses, as previously reported (figure 4F). We also observed instances, but only with MARC-T cells, where a single cell was able to lyse a target cell during the course of imaging. These observations may explain why MARC-T cells were more efficient than CAR-T cells in killing target cells with lower target densities (online supplemental figure S4H).

MARC-T cells efficiently eradicate leukemia, persist more, and are less exhausted than CAR-T cells

Considering the increase in stable immune synapse formation and cytolytic activity of MARC-T cells, we tested their efficiency for eradicating tumors in a cell line-derived xenotransplant model in NSG mice using NALM6-Luciferase. Primary human T cells transduced with either ZsGreen (Mock), CD19-targeting 28Z-CAR (CAR) or 28ZZ-MARC (MARC) were infused into mice 4 days after tumor transplant. Transferred Mock-T cells were unable to prevent tumor progression, with all mice having to be euthanized on day 22. Conversely, both CAR and MARC-T cells efficiently eradicated the tumor cells (figure 5A,B, online supplemental figure S5B). We recovered nearly twice as many MARC-T cells as CAR-T from the spleens of infused animals, suggesting an increase in either proliferation or persistence (figure 5C, online supplemental figure S5C). CAR and MARC-T cells also differed in their CD4/CD8 ratios, with CAR-T displaying a near 1:1 ratio between these subtypes, whereas MARC-T cells significantly favored CD8 T cells (online supplemental figure S5C). MARC-T cells displayed a significant reduction in PD1+ and LAG3+ frequencies, with differences in Tim3+frequencies approaching statistical significance (figure 5D, online supplemental figure S5D). In general, CAR-T cells displayed a significant increase in early and intermediately exhausted phenotypes, as demonstrated with the expression of either one or two exhaustion markers, when compared with MARC-T cells (online supplemental figure S5E). T cell exhaustion favored neither CD4 nor CD8 in any of the receptor-expressing T cells, with CAR-T similarly displaying increased exhaustion phenotype compared with MARC-T cells (figure 5E, online supplemental figure S5F).

As it is difficult to assess whether these differences may have resulted from natural variations across a small group of animals, we performed a similar study where both CAR- (ZsGreen) and MARC-T cells (mCherry) were coinjected in the same tumor-bearing animals, and tumor progression was monitored as before (figure 5F, online supplemental figure S5G,H). CAR/MARC-T infused mice rapidly controlled tumor growth and returned to baseline levels within days of treatment, whereas mice infused with control T cells failed to control tumor growth (figure 5G). Long-term protection of the CAR/MARC-T cells infused mice was determined by the absence of tumor growth following a rechallenge on day 28; all mice were able to control tumor transplant (online supplemental figure S5H). The mice were subsequently euthanized 4 weeks later, and CAR/MARC-T cell frequencies and phenotype were assessed (figure 5G). As observed in our previous in vivo assay, MARC-T cells significantly outnumbered CAR-T cells. Virtually, no CD8 CAR-T could be harvested from spleen or bone marrow (0.02% spleen, 0.0% BM) of the mice, whereas CD8 MARC-T cells were readily observed in the spleen (62%±24), but minimally in the BM (2.5%±0.3%) (figure 5H,I, online supplemental figure 5I,J). Finally, PD1+CD4 MARC-T cells were significantly less prevalent than CAR-T cells in both the spleen and BM (figure 5J,K, online supplemental figure S5L). Unfortunately, as there were little to no CD8 CAR-T cells, we could not do a comparison with MARC-T cells. On the other hand, PD1+CD8 MARC-T cells were significantly less prevalent than their CD4 counterparts in the spleen but not in the BM. Together, these results highlight the potency of the MARC-T cells, enabling efficient tumor eradication, all the while maintaining T cell functionality and persistence.

DISCUSSION

While CARs have revolutionized tumor-targeting immunotherapies, several limitations have hindered their effectiveness across diverse cancer types. A key shortcoming is the high tonic signaling observed in many 28ζ-derived CARs, independent of the hinge, TM domains, and scFv employed.[10] This tonic signaling often triggers early T cell exhaustion and restricts signaling dynamics after receptor engagement.[39] Primarily driven by the CD3ζ ITAMs, this signaling imbalance is influenced by the electrostatic properties of the CAR's cytoplasmic domains. Efforts to address this issue have included adding the cytoplasmic domain of CD3ε, in whole or part, to restore electrostatic balance.[12 31 32 40] Other groups have modified the CD3ζ ITAMs by either deleting ITAMs or by exchanging the functional tyrosines within them to phenylalanine in order to maintain the overall hydrophobicity of the motif while eliminating its ability to become phosphorylated.[41] While these strategies reduce tonic signaling, they often compromise receptor signaling potency.

We sought to create a modular chimeric antigen receptor akin to activating immune receptors by reproducing the same assembly requirements and modular context. Several studies have shown the potential of using activating KIR receptors as scaffolds for CARs (KIR-CARs). However, these scaffolds share signaling modules with other NK receptors often leading to limited surface expression due to competition for DAP12 utilization.[27 33] We first reasoned that by changing the position of the charged amino acid within the TM domains of both the RcMod and SigMod, we would be able to recreate a TAR

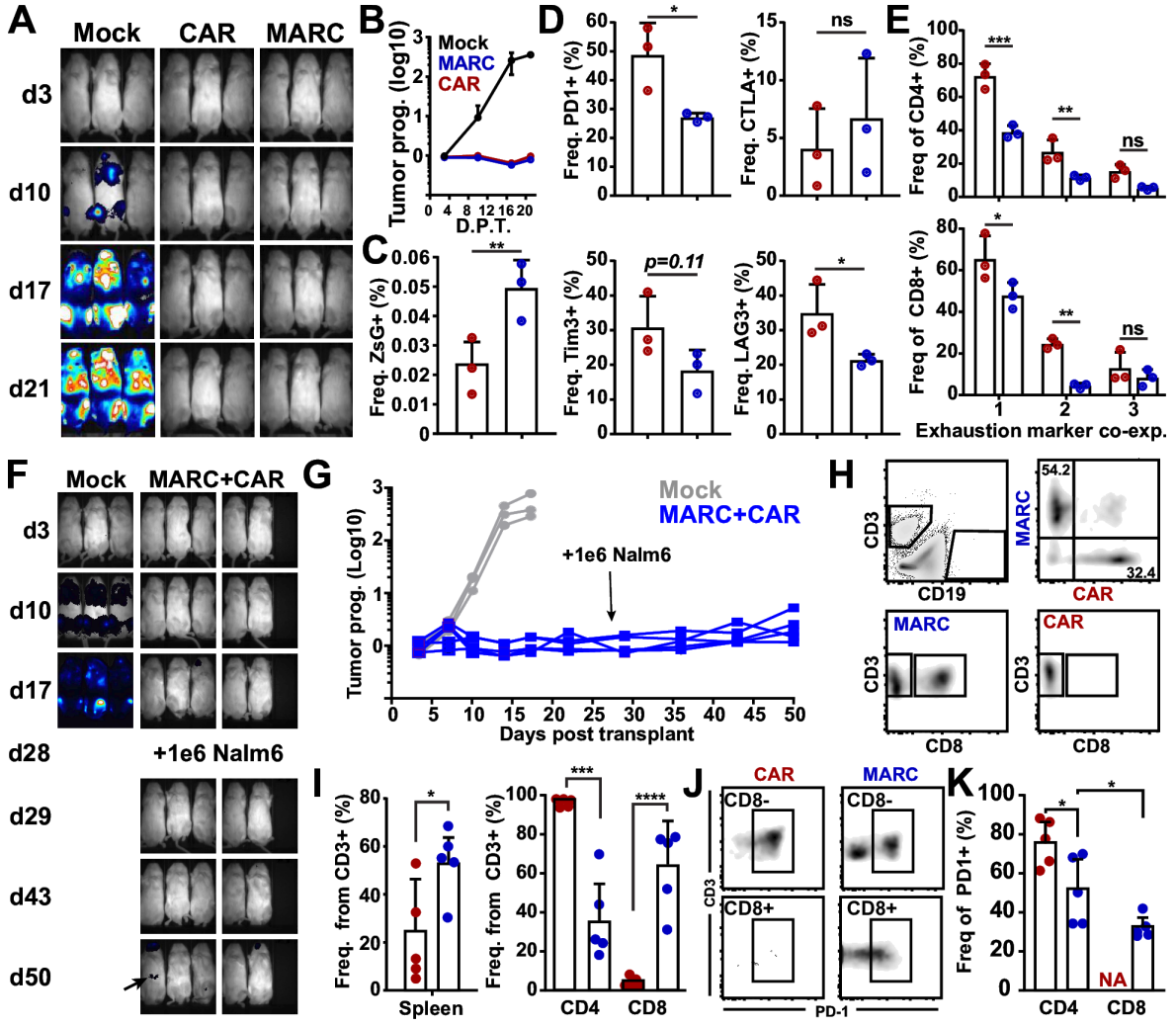

Figure 5 MARC-T cells are more persistent and display a less exhausted phenotype than CAR-T cells in an in vivo leukemia model. Control, CD19-targeting CAR or MARC-T cells were infused into NSG mice previously transplanted with 5e5 NALM6-Luc cells. Tumor burden was determined by imaging the mice at indicated days using the LabeoTech OiS300 in vivo imaging chamber. Mice were then sacrificed 1 day after the last images were taken, and T cells were harvested and analyzed. (A) Representative images showing tumor progression following the injection of D-Luciferin at various time points after tumor cell injections. Saturation point is set to $10e^8$ photons/s/cm^2. Three mice per group, front image capture. (B) Analyses of tumor progression as determined by fold change in Luciferase activity to non-tumor-bearing mice. Three mice per group. (C) Relative abundance of CAR and MARC T cells shown as ZsGreen+/ CD3+T cells fraction harvested from the mice at day 22, 3 mice per group. Statistical significance was determined using unpaired, two-way Student-t test. N=3. (D) Exhaustion phenotype of CAR and MARC-T cells as determined by staining for CTLA4, PD1, LAG3, and Tim3. Three mice per group. Statistical significance was determined using unpaired, two-way Student's t-test. (E) Analysis of coexpression of exhaustion markers expressed on CD4 (top) and CD8 (bottom) CAR and MARC-T cells. Three mice per group. Statistical significance of the frequency of one or multiple exhaustion markers between CAR and MARC was determined using two-way ANOVA with multiple comparisons, using Sidak post hoc test. (F) Representative images showing tumor progression following the injection of D-Luciferin at various time points after tumor cell injections. The saturation point is set to $10e^9$ photons/s/cm^2. At day 28, mice were rechallenged with 1e6 NALM6 and imaged for an additional 22 days. The arrow points to a potential early relapse in one of the mice. Five mice per group. (G) Analysis of tumor progression in mice as determined by fold change in Luciferase activity to non-tumor-bearing mice. At day 28, CAR/MARC-infused mice were rechallenged with 1e6 NALM6. Five mice per group. (H) FACS analyses showing the characterization and relative abundance of CAR and MARC-T cells based on CD3, CD19, and CD8 expression. Five mice per group. (I) Analyses displaying frequencies of CD4 and CD8 CAR and MARC from FACS data presented in H. Five mice per group. Statistical significance of the frequency of ZsGreen (CAR) or mCherry (MARC) cells within the CD3+population was determined using unpaired, two-way Student's t-test. Statistical significance of the frequency of CD4 or CD8 CAR or MARC-T cells was determined using two-way ANOVA with multiple comparisons, using Sidak post hoc test. (J) Exhaustion phenotype analyses in CD4 (CD8–) and CD8+CAR and MARC-T cells as determined by PD1 expression. (K) Analyses of PD1+frequencies in CD4 (CD8-) and CD8+CAR and MARC-T cells. Statistical significance of the frequency of PD1+cells from CD4 or CD8 CAR or MARC-T cells was determined using two-way ANOVA with multiple comparisons, using Sidak post hoc test. N=5. ANOVA, analysis of variance; MARC, Modular Actuation Receptor Complex.The p values are indicated as ns: non significant, ≤0.05: *, ≤0.01:**; 0.001:***, 0.0001:****.

capable of assembly with its registry-matched counterpart. Our findings revealed that while registry-matched TARs significantly enhanced assembly in both type I and type II RcMod architectures, residual assembly persisted in mismatched TARs. This phenomenon is consistent with other modular activating immune receptors integrating DAP12 or Fcγ, where TM positions mismatched by one helix turn still permit interaction.[17 42] The large side chain found in lysine may accommodate for such distant interactions. In addition, the presence of poly-leucine within our synthetic TAR (RS) may enable looser compaction of the TM helix bundle, also facilitating such interactions.[43 44] The overall hydrophobicity of the TARs, on the other hand, seems to dictate the requirement for assembly for surface expression (ie, the leakiness) of the RcMod. Indeed, in the context of the pL0 and pL4+, the RcMods were readily expressed at the surface in the absence of the SigMod. For instance, RcMods with pL0 and pL4+TARs showed high surface expression even without SigMods. Altering the amino acid at position 0' in the poly-leucine TAR demonstrated a strong correlation between hydrophobicity index and RcMod leakiness, except for histidine (figure 2G). Interestingly, this amino acid had already been tested in the context of modular receptors in previous studies but had failed to enable assembly in in vitro assays.[17] One feature found in histidine which may explain this is its ability to become protonated in acidic conditions and within the hydrophobic region of the cell membrane.[45 46] Protonation of histidine introduces a positive charge greatly changing its H.I. but may not occur in the restricted and controlled settings of in vitro assays, which may explain these discrepancies.

Optimization of the MARC's signaling capabilities was achieved by replacing the DAP12 cytoplasmic tail by that of CD3ζ, thereby increasing the total number of ITAMs from 2 to 6. This led to a more potent receptor capable of efficiently activating Jurkat T cells to levels comparable to that of CAR-expressing cells, despite its significantly lower surface density. The signaling kinetics of the MARC more closely resembled that of TCR-dependent signaling with rapid phosphorylation of receptor tyrosines and immediate downstream effector proteins such as ZAP70 and LAT. Intriguingly, within the MARC, the kinetics of CD28 phosphorylation were different from that of the CD3ζ ITAMs, which differs from previous findings with the 28Z-CAR using a phosphoproteomics approach.[12] Differences in signaling kinetics between the CD28 and CD3ζ moieties in the context of the MARC may become possible due to their presence on separate proteins, with each recapitulating the native topologies of endogenous receptors. Indeed, whereas activating immune receptors, such as the TCR, signal through their assembled SigMods, costimulatory proteins signal through the same polypeptide chain responsible for ligand binding. Another possibility for uncoupling the signaling kinetics of these components in the MARC is that the SigMod may become dissociated from the receptor during immune synapse formation, as observed for the CD3ζ component of the TCR.[47 48] Being physically separated from its RcMod, the CD3ζ-containing SigMod may differently encounter regulatory elements, such as phosphatases and ubiquitin ligases, thereby altering its state differently from that of the CD28 component of the RcMod. This could not occur in the context of a single-chain designed CAR.

The recapitulation of the native topologies of activating and costimulatory components with the MARC may also explain its lack of tonic signaling. It is now widely accepted that electrostatic interactions govern the signaling capabilities of ITAM-bearing SigMods, such as CD3ζ, CD3ε, Fcγ, DAP12, as well as costimulatory receptors such as CD28.[20 21 40 49] With native cytoplasmic domain sequences and topologies found in the MARC, the electrostatic signatures found within them are unaltered, which enable normal regulatory mechanisms to occur. Additionally, scFv-driven tonic signaling is also negated in the context of the MARC, as clearly demonstrated by the GD2-CARs, and CD33-CARs, potentially providing a greater safety profile than CARs for future treatment.[11] While the molecular mechanisms at play for negating scFv-driven tonic signaling were not directly assessed in this study, we hypothesize that the overall modular architecture of the MARC may prevent interchain refolding of the scFv by preventing proximity between distinct complexes within the PM. This, however, would have to be determined structurally in a follow-up study.

In vitro benchmarking further highlighted significant functional differences between CAR and MARC-T cells. Stable immune synapse formation, an important defect in CAR-T cells, was a common occurrence for MARC-T cells, which resulted in their ability to more efficiently kill target cells presenting lower target densities. We assert that the differences in synapse formation are intimately linked to the signaling dynamics of the MARCs; signaling dynamics shown to be defective in CAR-T cells.[12] This feature may become critical when integrating this technology for the treatment of solid tumors, where target expression heterogeneity and antigen escape are some of the more serious limitations of current CAR-T therapies. More importantly, the ability of a single MARC-T cell to kill its target may also ultimately lead to a reduction in CRS. Indeed, CAR-T cells typically require multiple transient interactions to lyse their target, due to the lack of stable immune synapse formation, and this leads to leaching of cytoplasmic content of the target cells, such as DNA and other DAMPs, into the environment prior to their death by apoptosis. This, in turn, is likely to trigger monocytes and neutrophils to engage the cytokine pathways associated with CRS.[50–53]

Significant differences between CAR and MARC-T cells were also observed in vivo. Our data clearly demonstrate that MARC-T cells surpassed CAR-T cells in many performance metrics. MARC-T cells outnumbered CAR-T and displayed significantly reduced exhaustion phenotypes in a clinically relevant mouse leukemia model. In our coinfusion and rechallenge model, MARC-T cells largely outnumbered CAR-T at 50+ days postinfusion, with the

CD8 CAR-T cells being virtually absent in the animals. MARC-T cells also displayed a significant reduction in the exhaustion marker PD1. The impact of negating tonic signaling in the MARC was beneficial to T cells and conflicts with the beneficial effect of low tonic signaling in CAR-T cell function in NCG mice in a previous study.[10] Although these models were significantly different, tonic signaling may represent a double-edged sword as TCR-based tonic signaling is near-absent in mouse models, and where CARs can substitute for this.[54] On the other hand, in patients where TCR-based tonic signaling is present, the added tonic signaling provided by CARs may become deleterious, thereby triggering early exhaustion and cell death often observed in the clinic. Insertion of CARs within the TCR locus, which eliminates TCR expression and its derived tonic signaling, has been shown to either be beneficial or deleterious to CAR-T cell health depending on the type of CAR used and its tonic signaling profile.[55 56]

Together, our work presents a novel architecture for cell-based immunotherapy that employs chimeric receptors synthetically recapitulating the topologies and assembly requirements of native immune receptors. Because these architectures and modes of assembly are shared among all immune cells, one could envision the design and optimization of the MARC for each type of effector immune cell. More work is needed to determine if CD28, or 4-1BB for that matter, are the optimal costimulatory signals to provide in this novel architectural setting and whether the MARC, with its lack of tonic signaling, would be more amenable to therapies based on hematopoietic stem cells (HSCs) or induced pluripotent stem cells (iPSCs). Indeed, CAR-HSC is the last frontier for cell-based immunotherapies enabling constant regenerative potential of immune effector cells. Designing optimal receptors for the desired immune effector cells and enabling lineage-specific expression in the context of CAR-HSC would usher in a new era for cancer immunotherapy.

MATERIALS AND METHODS

Generation of the MARCs

The KIR2DS3-derived MARC was built by fusing the CD19-specific single chain variable fragment (scFv) derived from the FMC63 monoclonal antibody to the first Ig domain of the extracellular domain of KIR2DS3 for each TAR tested, using overlap PCR. The DAPZ SigMod was generated by replacing the DAP12 intracellular domain by CD3z and was ordered at IDT as a Gblock. The CD8a-derived CARs and MARC were built by fusing the CD19-specific scFv (FMC63) to the extracellular domain of CD8a (T138). The CARs also used the CD8a TM domain and either CD3z or CD28-CD3z cytoplasmic domains. The MARC used the previously mentioned TARs and CD28 cytoplasmic domain, along with the registry-matched SigMods indicated in the figures.

Transduction of primary T cells

Our approach was based on published work by Gagliardi *et al*.[57] On day 0, peripheral blood mononuclear cells (PBMCs) were thawed in prewarmed TexMACS medium (Miltenyi Biotec) supplemented with 100 U/mL penicillin and 100 µg/mL streptomycin. Cells were plated at 2e6 cells/well in a 24-well G-REX plate (Wilson Wolf) and stimulated with soluble antibodies (Miltenyi Biotec): anti-CD3 (0.2 µg/mL), anti-CD28 (0.5 µg/mL) and cytokines (Miltenyi Biotec): human IL-7 (15 ng/mL) and human IL-15 (5 ng/mL) PBMCs were transduced 48 hours after stimulation, with a viral MOI of 4 using Vectofusin-1 (10 µg/mL final concentration) as per the manufacturer's protocol. The next day, TexMACS medium containing IL-7 and IL-15 was added to a final volume of 8 mL. Cytokines were added again every 2–3 days. Transduction efficiency was determined by analyzing ZsGreen fluorescence by flow cytometry on day 8 of primary T cell expansion. On day 9 of expansion, cells were counted and either frozen in CryoStor CS10 freezing solution (StemCell, 100-1061) or used directly for in vitro functional assays or NSG mouse infusions.

Onther materials and methods: online supplemental file 1

Author affiliations
[1]Département de microbiologie, Université de Montréal, Montreal, Quebec, Canada
[2]Université de Montréal Institut de Recherche en Immunologie et en Cancérologie, Montréal, Québec, Canada
[3]Modulari-T biosciences, Montréal, Quebec, Canada
[4]Médicine, Maisonneuve-Rosemont Hospital Research Centre, Montréal, Québec, Canada
[5]Département de médecine, Université de Montréal, Montréal, Québec, Canada
[6]Département de biologie et pathologie cellulaire, Université de Montréal, Montreal, Quebec, Canada
[7]Département de microbiobologie, infectriologie et immunologie, Université de Montréal, Montréal, Québec, Canada

Acknowledgements We thank IRIC In Vivo Biology and Flow Cytometry Core Facility employees for facilitating the in vivo experiments and analyses presented in this study. All animal studies were done in accordance with ethics approval. We'd like to thank Guy Sauvageau for reading the manuscript and providing insights.

Contributors AB-P, SM, DG, NF-K, LJ and BB performed experiments and analyzed data related to this study. JQ helped in the cloning of the various receptors tested. MKS-E-L oversaw the mouse experiments with the team of technicians at IRIC's mouse facility. J-SD helped with experimental designs and facilitated access to primary cell materials. MT and EG performed experiments, analyzed data and wrote the manuscript. EG is the guarantor. ChatGPT was used only to improve the concision and flow of the manuscript. Written text sections were submitted for improvement.

Funding This project was funded by CIHR operating grant (MOP-133726), LLSC New Idea award (LLS-567543) and CRS operating grant (OG-840622), as well as Stem Cell Network grant (SCN-C4R1-1).

Competing interests EG is cofounder and C.S.O. at Modulari-T biosciences and inventor of the patented technology showcased here.

Patient consent for publication Not applicable.

Ethics approval This study involves human participants and blood samples from humans were obtained from consenting patients based on our previous work and approvals by the research ethics committees of Héma-Québec and Hôpital Maisonneuve-Rosemont. Participants gave informed consent to participate in the study before taking part.

Provenance and peer review Not commissioned; externally peer reviewed.

Data availability statement All data relevant to the study are included in the article or uploaded as supplementary information.

ORCID iDs
Jean-Sebastien Delisle http://orcid.org/0000-0003-1460-7287
Etienne Gagnon http://orcid.org/0000-0001-5815-9768

REFERENCES

1 Hunger SP, Mullighan CG. Acute Lymphoblastic Leukemia in Children. *N Engl J Med* 2015;373:1541–52.
2 Grupp SA, Kalos M, Barrett D, *et al*. Chimeric antigen receptor-modified T cells for acute lymphoid leukemia. *N Engl J Med* 2013;368:1509–18.
3 Turtle CJ, Hanafi L-A, Berger C, *et al*. CD19 CAR-T cells of defined CD4+:CD8+ composition in adult B cell ALL patients. *J Clin Invest* 2016;126:2123–38.
4 Cappell KM, Kochenderfer JN. Long-term outcomes following CAR T cell therapy: what we know so far. *Nat Rev Clin Oncol* 2023;20:359–71.
5 Jain MD, Smith M, Shah NN. How I treat refractory CRS and ICANS after CAR T-cell therapy. *Blood* 2023;141:2430–42.
6 Brudno JN, Kochenderfer JN. Recent advances in CAR T-cell toxicity: Mechanisms, manifestations and management. *Blood Rev* 2019;34:45–55.
7 Calderon H, Mamonkin M, Guedan S. Analysis of CAR-Mediated Tonic Signaling. *Methods Mol Biol* 2020;2086:223–36.
8 Kouro T, Himuro H, Sasada T. Exhaustion of CAR T cells: potential causes and solutions. *J Transl Med* 2022;20:239.
9 Zhu X, Li Q, Zhu X. Mechanisms of CAR T cell exhaustion and current counteraction strategies. *Front Cell Dev Biol* 2022;10:1034257.
10 Qi C, Liu D, Liu C, *et al*. Antigen-independent activation is critical for the durable antitumor effect of GUCY2C-targeted CAR-T cells. *J Immunother Cancer* 2024;12:e009960.
11 Chen J, Qiu S, Li W, *et al*. Tuning charge density of chimeric antigen receptor optimizes tonic signaling and CAR-T cell fitness. *Cell Res* 2023;33:341–54.
12 Salter AI, Ivey RG, Kennedy JJ, *et al*. Phosphoproteomic analysis of chimeric antigen receptor signaling reveals kinetic and quantitative differences that affect cell function. *Sci Signal* 2018;11:eaat6753.
13 Call ME, Pyrdol J, Wiedmann M, *et al*. The organizing principle in the formation of the T cell receptor-CD3 complex. *Cell* 2002;111:967–79.
14 Call ME, Pyrdol J, Wucherpfennig KW. Stoichiometry of the T-cell receptor-CD3 complex and key intermediates assembled in the endoplasmic reticulum. *EMBO J* 2004;23:2348–57.
15 Call ME, Wucherpfennig KW. Molecular mechanisms for the assembly of the T cell receptor-CD3 complex. *Mol Immunol* 2004;40:1295–305.
16 Feng J, Garrity D, Call ME, *et al*. Convergence on a distinctive assembly mechanism by unrelated families of activating immune receptors. *Immunity* 2005;22:427–38.
17 Feng J, Call ME, Wucherpfennig KW. The assembly of diverse immune receptors is focused on a polar membrane-embedded interaction site. *PLoS Biol* 2006;4:e142.
18 Garrity D, Call ME, Feng J, *et al*. The activating NKG2D receptor assembles in the membrane with two signaling dimers into a hexameric structure. *Proc Natl Acad Sci U S A* 2005;102:7641–6.
19 Call ME, Wucherpfennig KW, Chou JJ. The structural basis for intramembrane assembly of an activating immunoreceptor complex. *Nat Immunol* 2010;11:1023–9.
20 Connolly A, Gagnon E. Electrostatic interactions: From immune receptor assembly to signaling. *Immunol Rev* 2019;291:26–43.
21 Dobbins J, Gagnon E, Godec J, *et al*. Binding of the cytoplasmic domain of CD28 to the plasma membrane inhibits Lck recruitment and signaling. *Sci Signal* 2016;9:ra75.
22 Bettini ML, Guy C, Dash P, *et al*. Membrane association of the CD3ε signaling domain is required for optimal T cell development and function. *J Immunol* 2014;193:258–67.
23 Xu C, Gagnon E, Call ME, *et al*. Regulation of T Cell Receptor Activation by Dynamic Membrane Binding of the CD3ε Cytoplasmic Tyrosine-Based Motif. *Cell* 2008;135:702–13.
24 Gagnon E, Xu C, Yang W, *et al*. Response multilayered control of T cell receptor phosphorylation. *Cell* 2010;142:669–71.
25 Li L, Guo X, Shi X, *et al*. Ionic CD3-Lck interaction regulates the initiation of T-cell receptor signaling. *Proc Natl Acad Sci U S A* 2017;114:E5891–9.
26 Liu W, Eilers M, Patel AB, *et al*. Helix packing moments reveal diversity and conservation in membrane protein structure. *J Mol Biol* 2004;337:713–29.
27 Wang E, Wang L-C, Tsai C-Y, *et al*. Generation of Potent T-cell Immunotherapy for Cancer Using DAP12-Based, Multichain, Chimeric Immunoreceptors. *Cancer Immunol Res* 2015;3:815–26.
28 Roseman MA. Hydrophobicity of the peptide C=O…H-N hydrogen-bonded group. *J Mol Biol* 1988;201:621–3.
29 Wimley WC, White SH. Experimentally determined hydrophobicity scale for proteins at membrane interfaces. *Nat Struct Biol* 1996;3:842–8.
30 Piechna K, Żołyniak A, Jabłońska E, *et al*. Activity and rational combinations of a novel, engineered chimeric, TRAIL-based ligand in diffuse large B-cell lymphoma. *Front Oncol* 2022;12:1048741.
31 Hartl FA, Beck-Garcìa E, Woessner NM, *et al*. Noncanonical binding of Lck to CD3ε promotes TCR signaling and CAR function. *Nat Immunol* 2020;21:902–13.
32 Wu W, Zhou Q, Masubuchi T, *et al*. Multiple Signaling Roles of CD3ε and Its Application in CAR-T Cell Therapy. *Cell* 2020;182:855–71.
33 Sun M, Xu P, Wang E, *et al*. Novel two-chain structure utilizing KIRS2/DAP12 domain improves the safety and efficacy of CAR-T cells in adults with r/r B-ALL. *Mol Ther Oncolytics* 2021;23:96–106.
34 Connolly A, Panes R, Tual M, *et al*. TMEM16F mediates bystander TCR-CD3 membrane dissociation at the immunological synapse and potentiates T cell activation. *Sci Signal* 2021;14:eabb5146.
35 Wu L, Brzostek J, Sakthi Vale PD, *et al*. CD28-CAR-T cell activation through FYN kinase signaling rather than LCK enhances therapeutic performance. *Cell Reports Medicine* 2023;4:100917.
36 Dong R, Libby KA, Blaeschke F, *et al*. Rewired signaling network in T cells expressing the chimeric antigen receptor (CAR). *EMBO J* 2020;39:e104730.
37 Wu L, Wei Q, Brzostek J, *et al*. Signaling from T cell receptors (TCRs) and chimeric antigen receptors (CARs) on T cells. *Cell Mol Immunol* 2020;17:600–12.
38 Díaz LR, Saavedra-López E, Romarate L, *et al*. Imbalance of immunological synapse-kinapse states reflects tumor escape to immunity in glioblastoma. *JCI Insight* 2018;3:e120757.
39 Ajina A, Maher J. Strategies to Address Chimeric Antigen Receptor Tonic Signaling. *Mol Cancer Ther* 2018;17:1795–815.
40 Wang H, Huang Y, Xu C. Charging CAR by electrostatic power. *Immunol Rev* 2023;320:138–46.
41 Feucht J, Sun J, Eyquem J, *et al*. Calibration of CAR activation potential directs alternative T cell fates and therapeutic potency. *Nat Med* 2019;25:82–8.
42 Blázquez-Moreno A, Park S, Im W, *et al*. Transmembrane features governing Fc receptor CD16A assembly with CD16A signaling adaptor molecules. *Proc Natl Acad Sci U S A* 2017;114:E5645–54.
43 Liu F, Lewis RNAH, Hodges RS, *et al*. Effect of variations in the structure of a polyleucine-based alpha-helical transmembrane peptide on its interaction with phosphatidylethanolamine Bilayers. *Biophys J* 2004;87:2470–82.
44 Grau B, Javanainen M, García-Murria MJ, *et al*. The role of hydrophobic matching on transmembrane helix packing in cells. *Cell Stress* 2017;1:90–106.
45 Wang Y, Park SH, Tian Y, *et al*. Impact of histidine residues on the transmembrane helices of viroporins. *Mol Membr Biol* 2013;30:360–9.
46 Parker JL, Li C, Brinth A, *et al*. Proton movement and coupling in the POT family of peptide transporters. *Proc Natl Acad Sci U S A* 2017;114:13182–7.
47 Kishimoto H, Kubo RT, Yorifuji H, *et al*. Physical dissociation of the TCR-CD3 complex accompanies receptor ligation. *J Exp Med* 1995;182:1997–2006.

48 Dumont C, Blanchard N, Di Bartolo V, *et al*. TCR/CD3 down-modulation and zeta degradation are regulated by ZAP-70. *J Immunol* 2002;169:1705–12.
49 Yang W, Pan W, Chen S, *et al*. Dynamic regulation of CD28 conformation and signaling by charged lipids and ions. *Nat Struct Mol Biol* 2017;24:1081–92.
50 Albelda SM. CAR T cell therapy for patients with solid tumours: key lessons to learn and unlearn. *Nat Rev Clin Oncol* 2024;21:47–66.
51 Lou H, Pickering MC. Extracellular DNA and autoimmune diseases. *Cell Mol Immunol* 2018;15:746–55.
52 Lachowicz-Scroggins ME, Dunican EM, Charbit AR, *et al*. Extracellular DNA, Neutrophil Extracellular Traps, and Inflammasome Activation in Severe Asthma. *Am J Respir Crit Care Med* 2019;199:1076–85.
53 Nath S, Roychoudhury S, Kling MJ, *et al*. The extracellular role of DNA damage repair protein APE1 in regulation of IL-6 expression. *Cell Signal* 2017;39:18–31.
54 Alcantar-Orozco EM, Gornall H, Baldan V, *et al*. Potential limitations of the NSG humanized mouse as a model system to optimize engineered human T cell therapy for cancer. *Hum Gene Ther Methods* 2013;24:310–20.
55 Stenger D, Stief TA, Kaeuferle T, *et al*. Endogenous TCR promotes in vivo persistence of CD19-CAR-T cells compared to a CRISPR/Cas9-mediated TCR knockout CAR. *Blood* 2020;136:1407–18.
56 Wang Z, Li N, Feng K, *et al*. Phase I study of CAR-T cells with PD-1 and TCR disruption in mesothelin-positive solid tumors. *Cell Mol Immunol* 2021;18:2188–98.
57 Gagliardi C, Khalil M, Foster AE. Streamlined production of genetically modified T cells with activation, transduction and expansion in closed-system G-Rex bioreactors. *Cytotherapy* 2019;21:1246–57.
58 Boudreau G, Carli C, Lamarche C, *et al*. Leukoreduction system chambers are a reliable cellular source for the manufacturing of T-cell therapeutics. *Transfusion* 2019;59:1300–11.